International Journal of Engineering & Technology Sciences
Volume 03, Issue 01, Pages 32-44, 2015
ISSN: 2289-4152

Design of High Performance LPF with Excellent Return Loss Using Stepped Impedance and Radial Resonators

Seyyed Mohammad Hadi Mousavi [a,b], Seyyed Vahab AL-Din Makki [b, c,*], Gh. Karimi [b,c]

[a] Department of Electrical Engineering, Kermanshah Science and Research Branch, Islamic Azad University, Kermanshah, Iran
[b] Department of Electrical Engineering, Kermanshah Branch, Islamic Azad University, Kermanshah, Iran.
[c] Department of Electrical Engineering, Faculty of Engineering, Razi University, Kermanshah, Iran.

* Corresponding author. Tel.: +989125091825;
E-mail address: v.makki@razi.ac.ir

Abstract

In this study, a novel microstrip lowpass filter (LPF) using stepped impedance, radial and open stub resonators is proposed. The insertion loss of the proposed filter is less than 0.4 dB in frequency range from DC up to 1.65 GHz. The transition band is from 1.796 up to 2.060 GHz with -3 and -40 dB attenuation points, respectively. LC equivalent circuit of the proposed main resonator is calculated precisely. The stopband bandwidth with a suppression factor of 25 dB is from 2.023 up to 15.14 GHz is reached; hence, a wide stopband with high suppression is accomplished. The results demonstrate that a roll-off rate of 140 dB/GHz, relative stopband bandwidth of 153% and a high figure-of-merit (FOM) of 24536 have been achieved. Furthermore, the proposed lowpass filter exhibits a small circuit of $0.097\lambda_g \times 0.225\lambda_g$ where λ_g is the guided wavelength at 3 dB cutoff frequency.

Keywords:

Microwave filters, Microstrip, Lowpass filter, Stepped impedance, T-shaped resonators, Sharp roll-off, Radial resonators.

Accepted:27 January2015

1. Introduction

High performance microwave filters with suitable specifications such as a sharp roll-off, wide stopband and good return loss are in demand for most wireless systems to suppress unwanted harmonics and noise. In recent years, a wide range of lowpass filters have been introduced, analyzed and implemented [3-9]. A microstrip lowpass filter with shunt open-stubs at the feed points of a center fed coupled-line hairpin resonator was analyzed and fabricated [3]. To reach a wider stopband, a lowpass filter using two closed loop stepped impedance (CLSI) and U-shape resonators was proposed [4]. In that paper, the proposed filter suffers from a gradual transition band. A structure using modified T-shaped resonators and spiral lines was proposed to achieve a better selectivity [6]. A compact lowpass filter using T-shaped resonator with a wide stopband was reported [5]. In the paper, a new microstrip lowpass with a compact circuit, good selectivity and ultra-wide stopband based on modified hairpin resonators was investigated. In another research, a lowpass filter using multiple polygonal resonators was presented [7]. In that paper, although a very good return loss was achieved, a good selectivity and relative stopband bandwidth was not suitable. Kaixue et al.

[8] proposed a new transformed radial stubs (TRSs) with a developed stopband. Other new methods like electromagnetic band-gap (EBG) and defected ground structure (DGS) [9] have been proposed.

In this study, a novel microstip lowpass filter with a sharp roll-off, wide stopband, excellent return loss and compact size based on stepped impedance resonators is proposed, fabricated and tested. The proposed structure has a cutoff frequency at 1.796 GHz and return loss better than 19 dB. The results indicate that the proposed LPF demonstrates a high figure-of-merit of 24536, while the suppression factor is better than 25 dB.

2. Filter Design Process

2.1. Lowpass filter design

Figure 1 shows the layout of the proposed LPF. Several stepped impedance, radial stub and open stub resonators are properly combined to achieve a LPF with excellent specifications. The proposed LPF is composed of four resonators which are clearly shown in Figure 1.

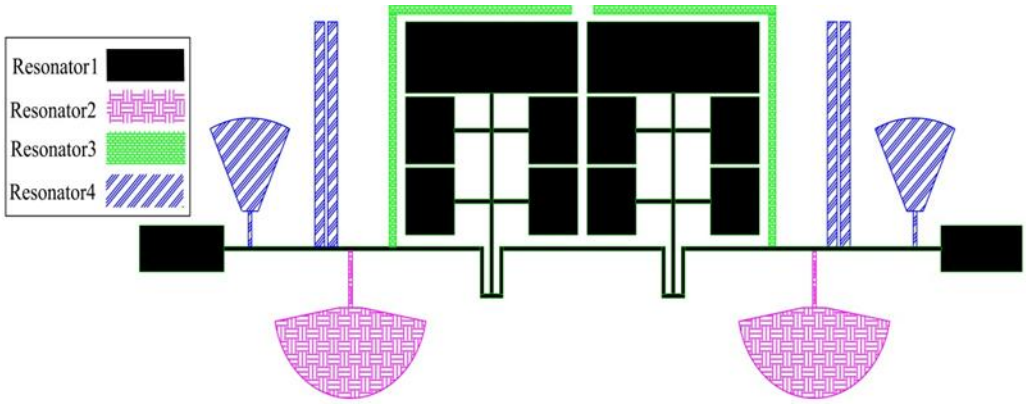

Fig.1: Layout of the proposed LPF

To investigate the design theory of the final LPF, we analyzed the resonators step by step. Resonator 1 is composed of a meandered transmission line and two basic resonators which are combined in series. According to Figure 2, it is obvious that by using the configuration, two additional deep transmission zeroes are generated. Using high-impedance meandered transmission lines instead of straight ones, reduces the circuit size and makes a narrower transition band.

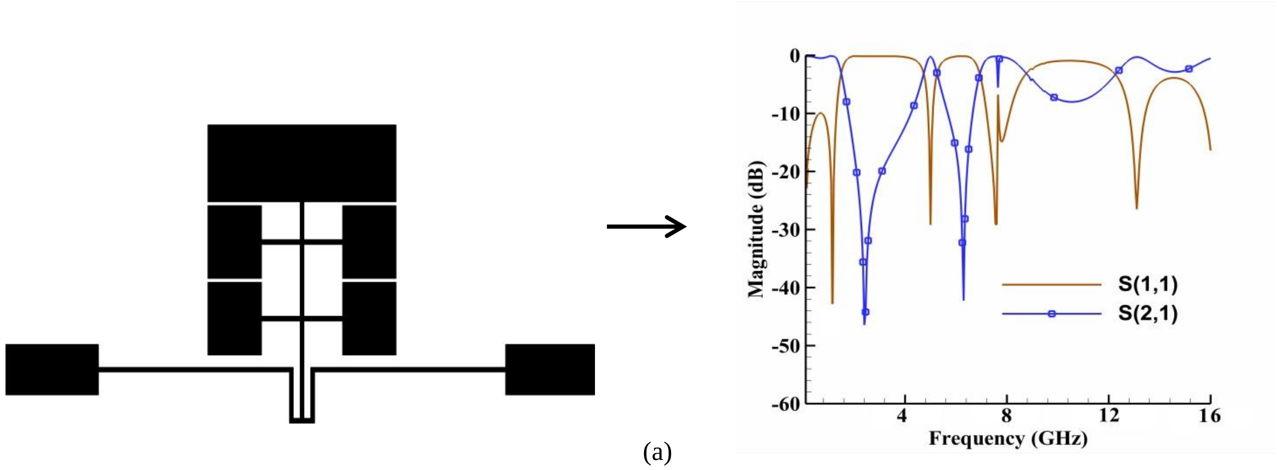

(a)

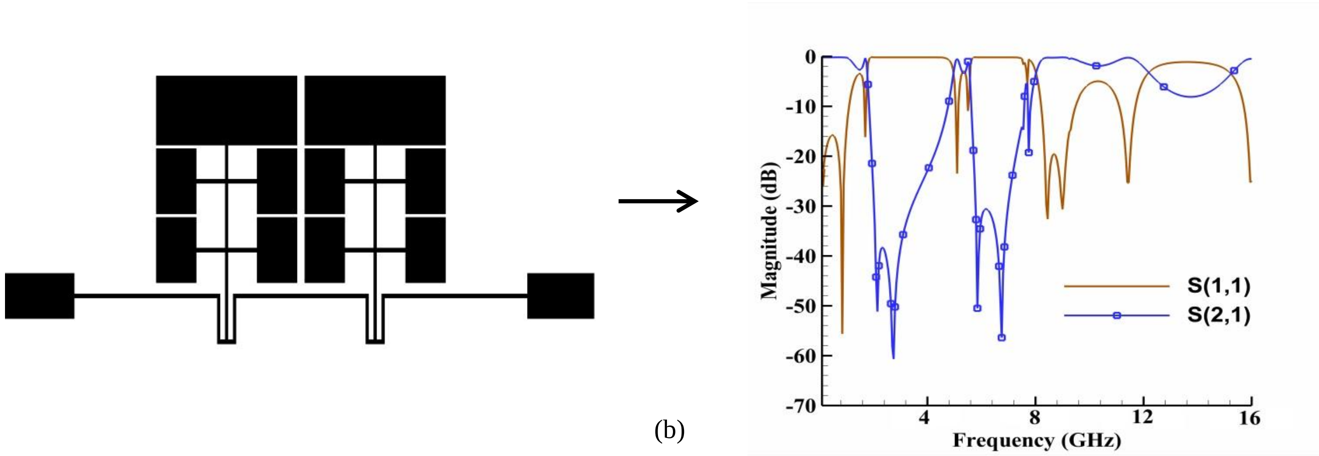

(b)

Fig.2: Process design of resonator 1, (a) The basic resonators. (b) Resonator 1

In order to achieve an impedance matching of 50 Ω, two rectangular patches as matching ports are connected to the input and output. Equations (1-4) can be used to calculate the width of matching ports. Where h and ε_r represent thickness and permittivity of the substrate, respectively, w is the width of the microstrip line and η equals to 120 ohms is the wave impedance in free space. All formulas have been discussed in [1].

For $w/_h \leq 1$:

$$\varepsilon_{re} = \frac{\varepsilon_r + 1}{2} + \frac{\varepsilon_r - 1}{2}\left\{\left(1 + 12\frac{w}{h}\right)^{-0.5} + 0.04\left(1 - \frac{w}{h}\right)^2\right\} \qquad (1)$$

$$Z_c = \frac{\eta}{2\pi\sqrt{\varepsilon_{re}}} ln\left(\frac{8h}{W} + 0.25\frac{W}{h}\right) \qquad (2)$$

For ${}^{W}/_{h} \geq 1$:

$$\varepsilon_{re} = \frac{\varepsilon_r + 1}{2} + \frac{\varepsilon_r - 1}{2}\left(1 + 12\frac{W}{h}\right)^{-0.5} \qquad (3)$$

$$Z_c = \frac{\eta}{\sqrt{\varepsilon_{re}}}\left\{\frac{W}{h} + 1.393 + 0.667\, ln\left(\frac{W}{h} + 1.444\right)\right\}^{-1} \qquad (4)$$

Figure 3 depicts the layout of resonator 1. The dimensions of resonator 1 are as follows: d1= 1.17 mm, d2= 2.6 mm , d3= 7.9 mm, d4= 4.9 mm, d5 =1.1 mm, d6= 1.1 mm, d7= 1.7 mm, d8= 0.9 mm, d9= 1.2 mm, d10= 1.7 mm ,d11= 1.5 mm, d12= 2.4 mm , d13= 0.7 mm ,d14= 0.1 mm, d15= 5.3 mm, d16= 1.8 mm, d17= 22.1 mm, g1= 0.3 mm, g2= 0.1 mm, g3= 0.1 mm, g4= 0.2 mm, and g5= 0.3 mm.

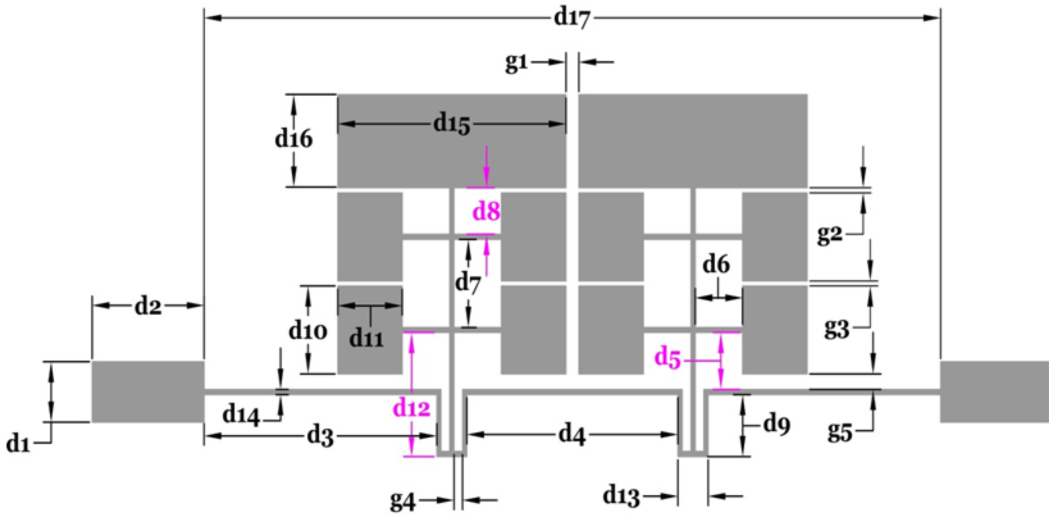

Fig.3: Resonator 1

Resonator 1 and its S-parameters are shown in Figure 2(b), which generates four transmission zeroes at 2.123, 2.741, 5.856, and 6.750 GHz with the attention levels of -52.2, -61.4, -51.8, and -56.5 dB, respectively. Figure 2(b) clearly shows by generating two transmission zeroes close to the cutoff frequency, a very sharp transition band is achieved. The third and fourth transmission zeroes are used to develop the width of the stopband. In order to analyze resonator 1, the LC model of resonator 1 is utilized and calculated precisely. Figure 4(a) and (b) depict the LC model of resonator 1 and a comparison between EM-simulation and LC-simulation, respectively.

.

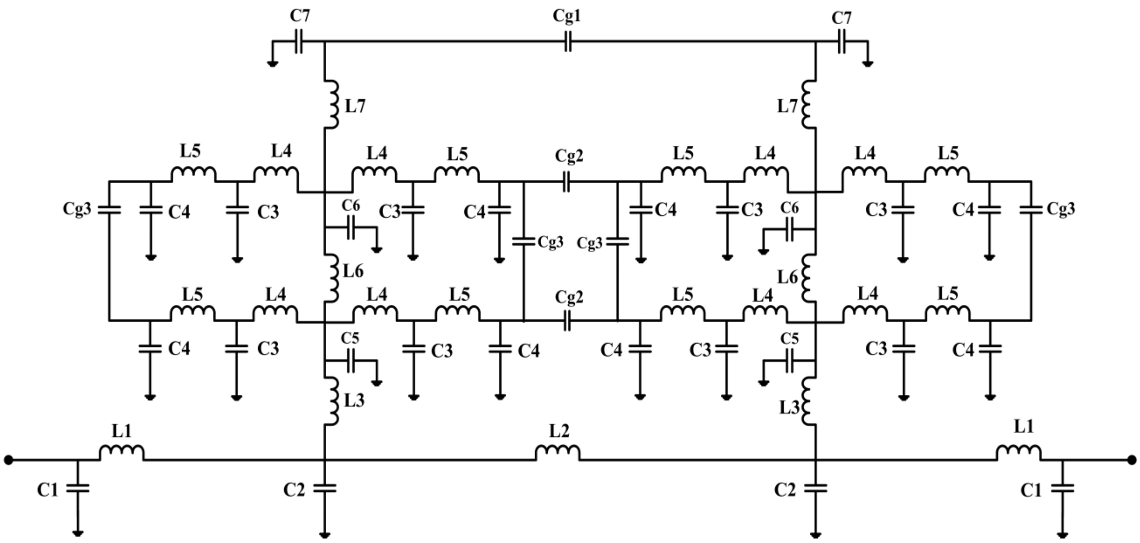

(a)

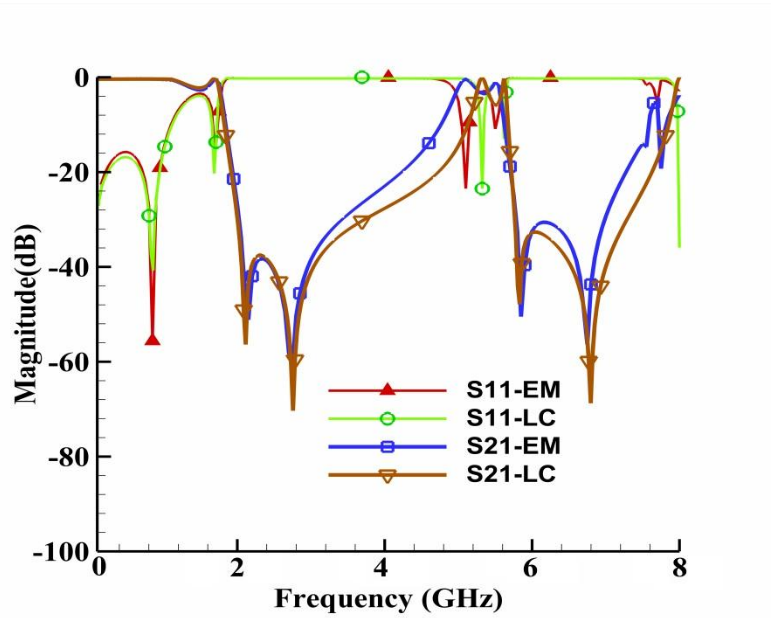

(b)

Fig.4: LC model of resonator 1, (a) Proposed LC model. (b) LC and EM simulation results

According to Figure 4, a very good similarity between LC-simulation and EM-simulation is accomplished which indicates an important achievement. The values of the inductances and capacitances are as follows: L1= 6.3 nH, L2= 5.34 nH, L3= 1.735 nH, L4= 0.8 nH, L5= 0.32 nH, L6= 1.3 nH, L7= 0.17 nH, C1= 0.17 pF, C2= 0.35 pF, C3= 0.125 pF, C4= 0.1 pF, C5= 0.11 pF, C6= 0.39 pF, C7= 0.3 pF, Cg1= 0.02 pF, Cg2= 0.02pF, and Cg3= 0.03pF.

L1 and L2 are the inductances C2 is the capacitance of the transmission line and C2 is the sum of the transmission line capacitance and a part of high-impedance line. L3, L4, L5, L6, L7, and C3, C6 are inductances and capacitances of the high and low-impedance lines. C4 and C7 are the sum of the capacitances of open-ends and low impedance lossless lines. Cg1 and Cg2 are the capacitance with the width of g1. Cg3 is the gap capacitance with the width of g3. Other gaps with width of g2 g5 because of the low effect are ignored. A low and high-impedance lossless line terminated at both ends with relatively low impedance lines can be investigated by a Π-equivalent circuit, as shown in Fig.5. The values of inductors and capacitors can be attained as:

$$l_s = \frac{1}{\omega} \times Z_s \times \sin\left(\frac{2\pi}{\lambda_g} l\right) \qquad (5)$$

$$C_s = \frac{1}{\omega} \times \frac{1}{Z_s} \times \tan\left(\frac{\pi}{\lambda_g} l\right) \qquad (6)$$

Formulas of open-end have been discussed in [1]. Also the structure and equivalent circuit are shown in Figure 6. As shown in Figure 7. A microstrip gap can be represented by an equivalent circuit; all formulations are referenced in [10].

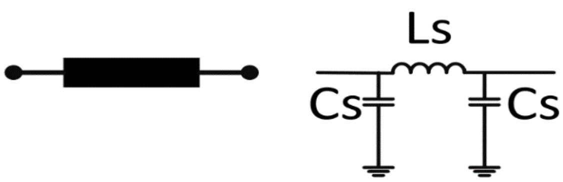

Fig. 5: Layout and equivalent LC circuit of high and low-impedance lossless line

Fig. 6: Layout and equivalent LC circuit of open-end

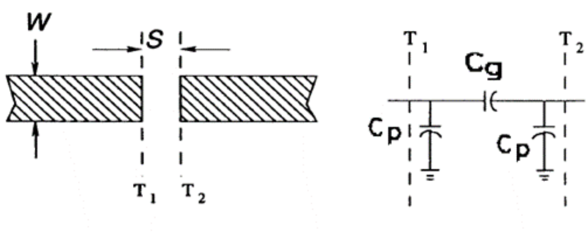

Fig. 7: Layout and equivalent LC circuit of a microstrip gap

According to the Figure 2(b), resonator 1 has a narrow stopband bandwidth. In order to suppress harmonics in the stopband, resonator 2 is added to resonator 1. Figure 8 (a) and (b) show the layout of resonator 1 in combination with resonator 2 and its S-parameters, respectively. The dimensions of the resonator 2 are shown in Figure 8 (a) are as follows: d18= 2 mm, d19= 0.1 mm, d20= 0.7 mm, d21= 1.45 mm, d22= 3.95 mm, d23= 3.85 mm, and D1=160°.

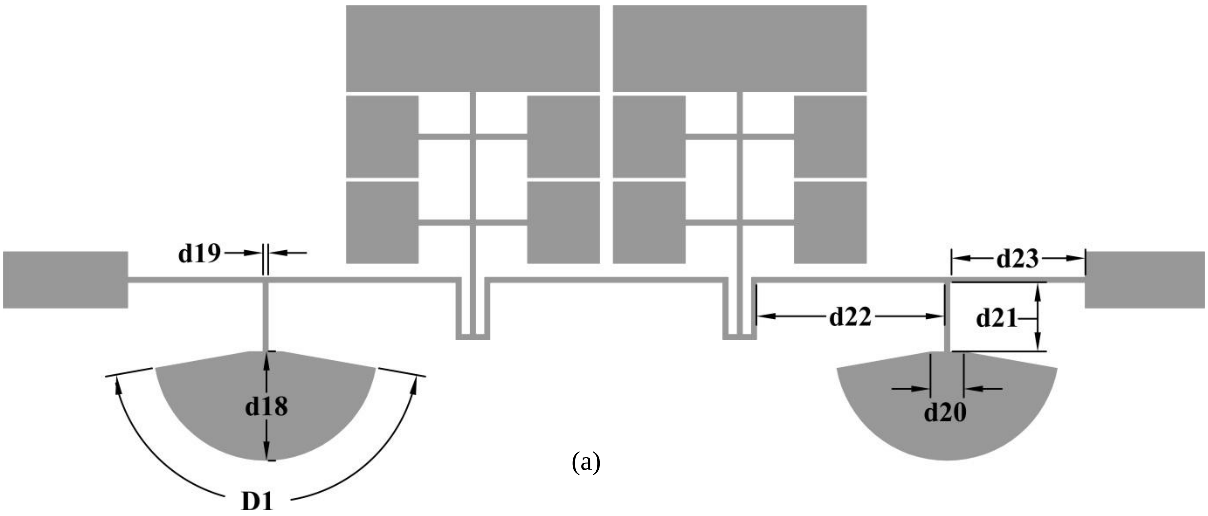

(a)

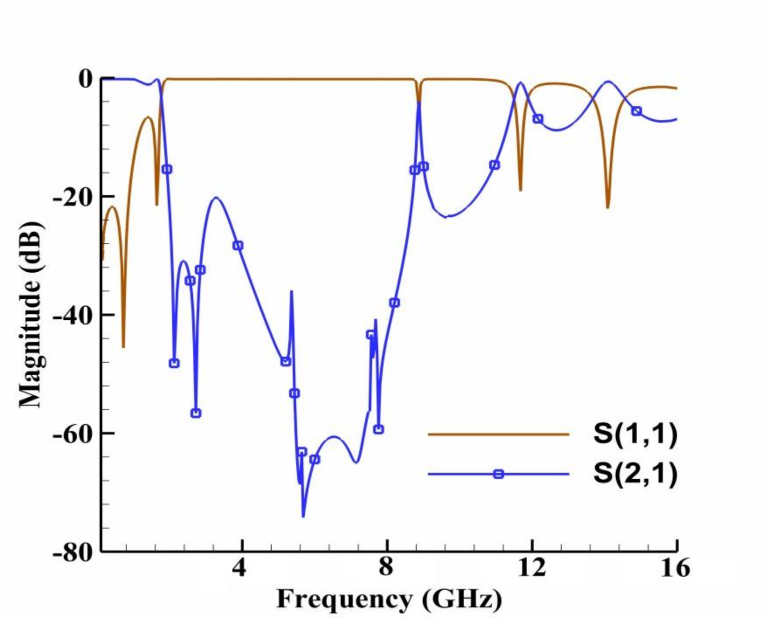

(b)

Fig.8: Resonator 1 in combination with resonator 2, (a) Layout. (b) S-parameters

As seen in Figure 8(a) and (b), resonator 3 is composed of two high-impedance lines loaded by radial stub resonators. By using the structure, a wider stopband from 3 up to 8 GHz is reached, but other specifications still need improvement. In order to develop the stopband, transmission peaks should be rejected by employing some transmission zeroes generated by suitable suppressing cells. So, to improve the sharpness and the insertion loss, two folded open stubs namely resonator 3 are employed. Figure 9(a) and (b) show resonator 1 in combination with resonator 2 and 3, and its frequency response, respectively. Parameters of resonator 3 are as follows: d24= 6.1 mm, d25= 5.6 mm, d26= 0.2 mm, d27= 5.1 mm, d28= 2.6 mm, g6= 0.7 mm, and g7= 0.3 mm.

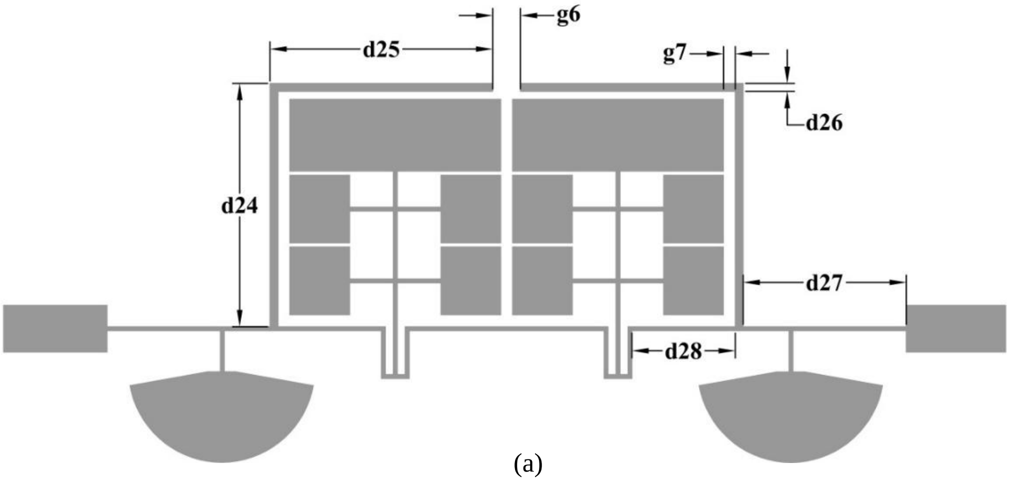

(a)

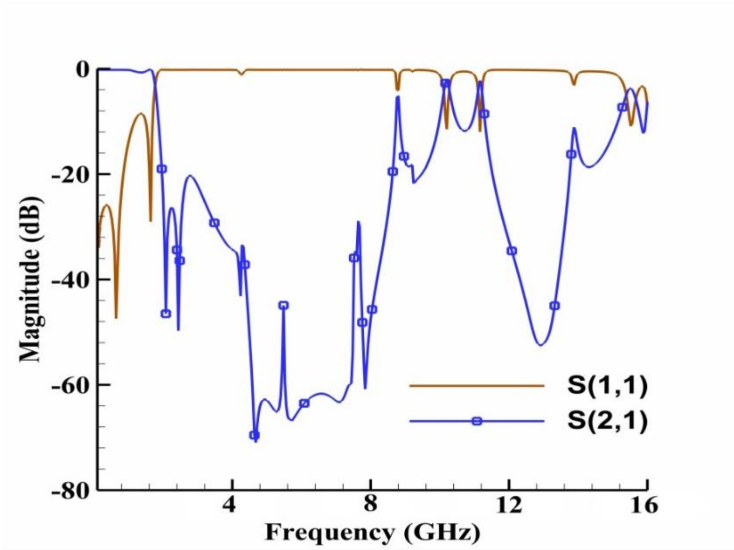

(b)

Fig.9: Resonator 1 in combination with resonator 2 and 3, (a) Schematic diagram. (b) S-parameters

Figure 9(b) clearly shows by adding resonator 3, the selectivity and the insertion loss are improved. additionally, a deep transmission zero at 12.91 GHz with the attention level of -52.4 dB is generated. Although resonators 1, 2 and 3 have created an acceptable selectivity, they have not a wide stopband. In order to suppress undesirable harmonics, in final step, four open stubs and two high impedance lines loaded by radial stub resonators are adopted. Figure 10 (a) and (b) show the final filter and its S-parameters. Parameters of resonator 4 are as follows: d29=5.7 mm, d30= 0.3 mm, d31= 2.3 mm, d32= 0.75 mm, d33= 0.9 mm, d34= 1.6 mm, d35= 2.8 mm, d36= 0.5 mm, d37= 0.1 mm, g8=0.1 mm, and D2= 50°.

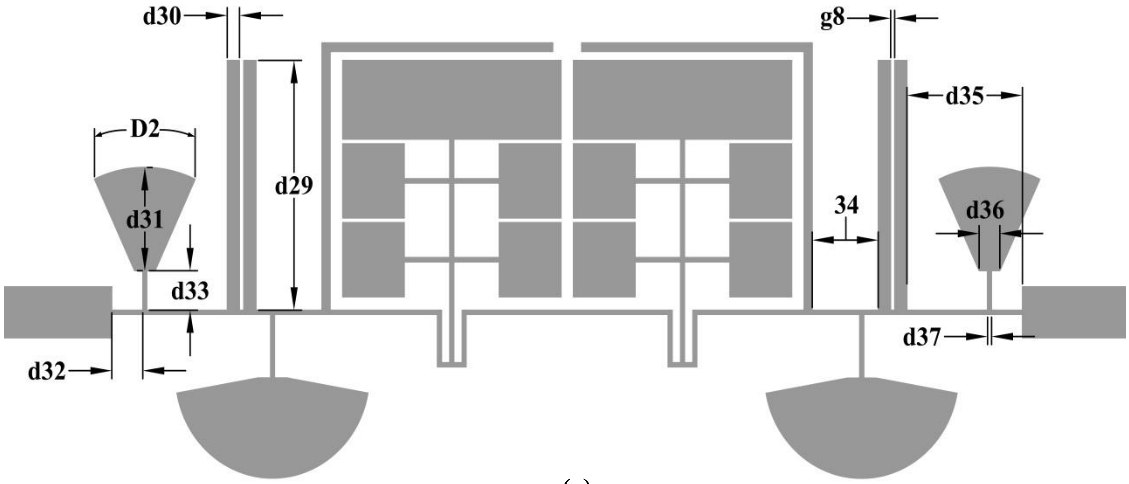

(a)

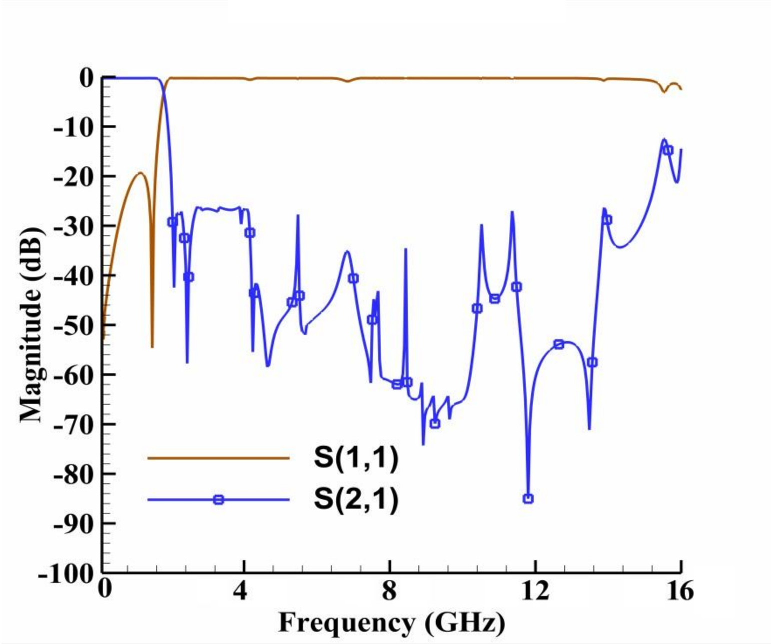

(b)

Fig.10: The final LPF, (a) Layout of the final filter. (b) S-parameters

According to Figure 10 (b), it is obvious that by adding resonator 4 the insertion loss, return loss and suppression factor have improved significantly and a wide stopband together with a high suppression in this frequency range are accomplished.

2.2. Voltage standing wave ratio (VSWR)

One the most important features of the proposed LPF is that the proposed filter can achieve a high figure-of-merit (FOM) while a very good return loss and VSWR are obtained. The proposed bended transmission line in this configuration not only reduces the size of the LPF, but also decreases VSWR (Voltage Standing Wave Ratio). When a signal is transmitted via a frequency-selective network like a filter, some delay is introduced into the output signal in relation to the input signal [2]. The parameter Γ is also called the reflection coefficients. VSWR can be given by:

$$RL = -20\log|\Gamma| \;\; dB \quad (7)$$

$$VSWR = \frac{1+|\Gamma|}{1-|\Gamma|} \quad (8)$$

Note that in a matched load $\Gamma = 0$ and return loss is ∞ ; in a mismatched load $\Gamma = 1$ and return loss is 0 dB. As seen from Table 1 that by increasing the width of the d9 (see Figure 3), a smaller VSWR is achieved.

Table 1: Effect of d9 on VSWR

d9	Return loss(RL)	**Γ**	VSWR
0.0 mm	13.9	0.202	1.506
0.5 mm	15.10	0.176	1.427
0.9 mm	17.2	0.138	1.320
1.2 mm (This letter)	19	0.112	1.253

3. Simulation and measurement S-parameters

The proposed LPF has been designed and fabricated on a Rogers 4003 with relative dielectric constant of 3.38, thickness of h=20 mil and loss tangent equal to 0.0022. The S-parameters is measured by using HP8757A network analyzer. The results indicate that the fabricated filter has a cutoff frequency equals to 1.796 GHz and narrow transition band from 1.796 up to 2.060 GHz (with -3 and -40 dB suppression level) which is represents a quick transition. In the passband region, maximum insertion loss is less than 0.5 dB and the return loss is better than 19 dB, which is considered as an excellent achievement. The stopband band width is from 2.023 up to 15.14 GHz with 25 dB suppression factor, therefore, the proposed LPF can achieve a relative stopband bandwidth of 153%. The size of the lowpass filter is only 9.9 ×22.9 mm^2 which corresponds to 0.097 λ_g ×0.225λ_g. Table 2 depicts a performance comparison among this letter and some other letters. The photograph and measured results are shown in Figure 11(a) and (b).

Among them, the roll-off rate is given by:

$$\xi = \frac{\alpha_{\max} - \alpha_{\min}}{f_s - f_c} (dB / GHz) \quad (9)$$

where $\alpha_{\max}$ is the 40 dB attenuation point, $\alpha_{\min}$ is the 3 dB attenuation point, f_s is the 40 dB stop-band frequency, and f_c is the 3 dB cutoff frequency. The relative stopband bandwidth (RSB) is calculated by:

$$RSB = \frac{stopband \quad bandwidth}{stopband \quad center \quad frequency} \quad (10)$$

The suppression factor (SF) is based on the stopband rejection degree. For instance, the rejection level referred to 25 dB suppression, thus the corresponding SF is defined as 2.5. The normalized circuit size (NCS) is calculated by:

$$NCS = \frac{physical \quad size \quad (length \times width)}{\lambda_g^2} \quad (11)$$

Where λ_g is the guided wavelength at 3 dB cutoff frequency. The architecture factor (AF) can be recognized as the circuit complexity factor. Finally, figure-of-merit (FOM) as overall index is given by:

$$FOM = \frac{\xi \times RSB \times SF}{NCS \times AF} \quad (12)$$

Table 2: Performance comparison among published filters and presented one

Ref.	RO	RSB	SF	AF	NCS	FOM
[3]	95	1.40	2	1	0.104×0.214	11951
[4]	80.43	1.64	2.3	1	0.330×0.180	5108
[5]	46	1.37	2	1	0.220×0.137	4182
[6]	105	1.47	2	1	0.312× 0.110	8994
[7]	58.6	1.43	2.5	1	0.22× 0.11	8657
[8]	62	1.72	3	1	0.310×0.240	4430
Our work	140	1.53	2.5	1	0.225×0.097	24536

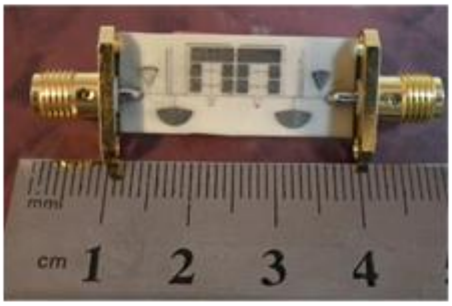

(a)

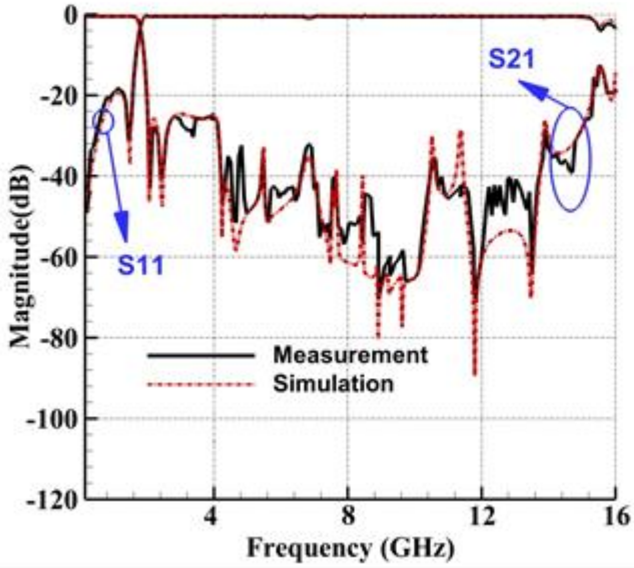

(b)

Fig.11: Fabricated LPF, (a) Photograph. (b) Measurement and simulation results

4. Conclusion

A new compact microstip lowpass filter consisting of a high impedance transmission line, two radial and multiple open stubs has been designed and implemented. The results indicate that the presented LPF can accomplish several outstanding characteristics. The cutoff frequency equals to 1.796 GHz, while a sharp roll-off rate of 140 dB/ GHz is achieved.

References

[1] Hong JS, Lancaster MJ. Microstrip filters for RF/microwave applications. New York: Wiley 2011; 2nd, E.

[2] Pozar DM. Microwave Engineering, New York: Wiley 1998; 2nd, E.

[3] Velidi VK, Sanyal S. Sharp roll-off lowpass filter with wide stopband using stub-loaded coupled-line hairpin unit. *IEEE Microwave and Wireless Components Letters* 2011; 21(6): 301–303.

[4] Lotfi S, Makki SVA, Majidifar S. Design of microstrip lowpass filter with ultra-wide stopband and sharp rejection. *International Journal of Engineering & Technology Sciences (IJETS)* 2014; 2(1): 47–57.

[5] Sariri H, Rahmani Z, Lalbakhsh A, Majidifar S. Compact LPF using T-shaped resonator. *Frequenz* 2013; 67(1-2): 17–20.

[6] Hookari M, Karimi Gh. Design of microstrip filter using modified T-shaped with wide stopband. *International Journal of Engineering & Technology Sciences (IJETS)* 2014; 2(2): 138–145.

[7] Mirzaee M, Virdee B.S. Realisation of highly compact planar lowpass filter for UWB RFID applications. *Electronic Letters* 2013; 49 (22):1396–1398.

[8] Kaixue Ma, Yeo K.S. New ultra-wide stopband low-pass filter using transformed radial stubs. *IEEE Trans. Microw. Theory Tech* 2011; 59 (3): 604–611.

[9] Al Sharkawy M. H, D. Abd El-Aziz D, Mahmoud G. A miniaturized lowpass/bandpass filter using double arrow head defected ground structure with centered etched ellipse. *Progress In Electromagnetics Research Letters* 2011; 24: 99–107.

[10] Gupta K. C, Ramesh G, Bahl I, Bhartia P. Microstrip Lines and Slotlines. Boston: Artech House Publishers; 1996; 2nd, E.